Published as: *J Immunol*. 2008 November 15; 181(10): 6850–6858.

Polysialic acid, a glycan with highly restricted expression, is found on human and murine leukocytes and modulates immune responses[1]

Penelope M. Drake[*], **Jay K. Nathan**[*], **Christina M. Stock**[*], **Pamela V. Chang**[*], **Marcus O. Muench**[§], **Daisuke Nakata**[¶], **J. Rachel Reader**[‖], **Phung Gip**[†], **Kevin P.K. Golden**[*], **Birgit Weinhold**[#], **Rita Gerardy-Schahn**[#], **Frederic A. Troy II**[¶], and **Carolyn R. Bertozzi**[*,†,‡]

[*]Department of Chemistry, University of California, Berkeley

[§]Blood Systems Research Institute, San Francisco, California and Department of Laboratory Medicine, University of California, San Francisco

[¶]Department of Biochemistry and Molecular Medicine, School of Medicine, University of California, Davis

[†]Department of Molecular and Cell Biology, University of California, Berkeley

[#]Abteilung Zelluläre Chemie, Zentrum Biochemie, Medizinische Hochschule Hannover, Germany

[‡]Howard Hughes Medical Institute, San Francisco, California and Department of Laboratory Medicine, University of California, San Francisco

[‖]The Comparative Pathology Laboratory, School of Veterinary Medicine, University of California, Davis

Abstract

Polysialic acid (polySia) is a large glycan with restricted expression, typically found attached to the protein scaffold neural cell adhesion molecule (NCAM). PolySia is best known for its proposed role in modulating neuronal development. Its presence and potential functions outside the nervous systems are essentially unexplored. Here we show the expression of polySia on hematopoietic progenitor cells, and demonstrate a role for this glycan in immune response using both acute inflammatory and tumor models. Specifically, we found that human NK cells modulate expression of NCAM and the degree of polymerization of its polySia glycans according to activation state. This contrasts with the mouse, where polySia and NCAM expression are restricted to multipotent hematopoietic progenitors and cells developing along a myeloid lineage. Sialyltransferase (ST) 8Sia IV-/- mice, which lacked polySia expression in the immune compartment, demonstrated an increased contact hypersensitivity response and decreased control of tumor growth as compared to wild-type animals. This is the first demonstration of polySia expression and regulation on myeloid cells, and the results in animal models suggest a role for polySia in immune regulation.

[1]The research was made possible by a grant from the California Institute for Regenerative Medicine (Grant Number RS1-00365). The contents of this publication are solely the responsibility of the authors and do not necessarily represent the official views of CIRM or any other agency of the State of California.

Authorship: PD conceived, and helped to perform and analyze all experiments. JN carried out immunoblotting and in vivo immunoassays. CS and KG executed in vivo immunoassays. PC performed 5'FU assays and flow cytometric analyses of perpherial myeloid cells. MM designed and executed in vitro colony-forming assays. DN and FAT performed the DP analysis. RR provided pathological evaluation of ear sections. PG prepared and analyzed human NK cells. BW and RGS provided transgenic mice, mAb 735 and EndoN. PD and CB wrote the manuscript.

Keywords

Natural Killer Cells; Neutrophils; Hematopoiesis

Introduction

Polysialic acid (polySia) is an unusual glycan by almost any definition. Structurally, it comprises repeating sialic acid monomers with α2,8 linkages. Its size in terms of monosaccharide units, or degree of polymerization (DP), is large, with reported values of 50–150 ranging up to >370 residues (1,2). This contrasts with the typical N-linked glycan containing 10–12 monomers, and is similar to glycosaminoglycans (GAGs), which average 80–100 residues (3). The synthesis of polySia is also unusual—an entire chain is produced by a single enzyme acting on classical N-linked, and less commonly, O-linked core structures. Two polysialyltransferases, ST8Sia IV (PST) and ST8Sia II (STX), with distinct expression patterns are involved in synthesis of polySia. In contrast, the synthesis of most glycans requires the coordinated action of many enzymes. Therefore, while glycan structure is difficult to track genetically, polySia can be localized by the expression patterns of ST8Sia IV and ST8Sia II. Furthermore, while many glycan structures can modify any number of protein cores, the polysialyltransferases appear to be highly selective in their scaffold choices. Aside from autopolysialylation of the ST8Sia IV and ST8Sia II enzymes, only four other protein carriers have been identified: the neural cell adhesion molecule (NCAM, also termed CD56), the α-subunit of the voltage-gated sodium channel, CD36 and neuropilin (4–7). Of these, NCAM is by far the most commonly used scaffold.

Polysialylated NCAM is prominent in the developing nervous system, where it has been most extensively studied. A large body of work has shown that polySia affects neuronal functions as varied as migration (8,9), cytokine response (9,10) and cell contact-dependent differentiation (11). Provocatively, these same functions are vital components of immune function. Leukocytes migrate throughout the body, guided by specialized cytokines, termed chemokines, to effect both homeostatic and inflammatory functions that are often dictated through cytokine and cell contact-dependent signals.

Intriguingly, expression of both ST8Sia IV and ST8Sia II has been documented in the immune system, suggesting that polySia is abundant therein. In the adult human, primary and secondary lymphoid organs including the placenta, spleen, thymus, intestine, and peripheral blood express ST8Sia IV, while ST8Sia II is produced in the thymus (12). Our recent work in the mouse suggests that polySia plays an important role in progenitor trafficking to the thymus (manuscript in preparation). Furthermore, NCAM (CD56) is expressed on two subsets of mature human lymphocytes: natural killer (NK) cells and natural killer T (NKT) cells. Although NCAM has long been used as a marker for these cell populations (13), its functional role remains undefined. We postulated that in the immune system NCAM functions as a scaffold for presentation of polySia, and that the glycan itself confers function to this glycoprotein. Moreover, the functional significance of these observations is unknown.

The documented role of polySia in modulating cell adhesion, migration and cytokine response in the nervous system motivated us to investigate the possibility of analogous functions in the immune system. Here, we describe polySia expression on NCAM in human NK cells, as well as mouse hematopoietic progenitors and myeloid cells. In support of a role for polySia in the immune system, we demonstrate that human NK cells regulate the expression and length of polySia with activation state, and that ST8Sia IV-/- mice have aberrant contact hypersensitivity responses and enhanced tumor growth as compared to wild-type mice.

Materials and Methods

Mice

Wild-type C57Bl/6 and congenic GFP+ mice were purchased from Jackson Labs. Mice were housed in specific pathogen-free conditions. Experiments were approved by UC Berkeley's Animal Care and Use Committee. The generation of ST8Sia IV-/- and ST8Sia II-/- mice has been described (14,15).

Human NK-cell analysis

Human leukocytes were obtained as buffy coats from the American Red Cross, Oakland, CA. PBMCs were prepared as described (16). NK cells were isolated using a magnetic bead-based method (Dynal NK Cell Negative Isolation Kit, Invitrogen; Carlsbad, CA). Cells were either lysed directly, or cultured in RPMI with 10% FBS. Endoneuraminidase N (EndoN) (1:1000 – 1:2000 dilution) and/or 6000 U/mL recombinant IL-2 (NCI Preclinical Repository) were added as indicated.

Human bone marrow analysis

Human fetal bone marrow was obtained from elective pregnancy terminations at the University of California San Francisco with approval of the Committee for Human Research. Bone marrow was harvested from long bones as previously described (17). Light-density cells were isolated by centrifugation on a layer of 1.077 g/ml NycoPrep (Axis-Shield PoC AS, Oslo, Norway). Both total and light-density cell fractions were studied.

Assessment of polySia polymerization

Human NK cell cultures were pelleted, flash frozen, and stored at −80 °C until analysis. Pellets from five individual donors were combined, and the degree of polymerization was determined as described (2).

Antibodies

Antibodies used for flow cytometry are as follows. From eBioscience (San Diego, CA): fluorescein-conjugated anti-CD3ε (145-2C11), anti-CD4 (GK1.5), anti-CD11b (M1/70), anti-CD25 (PC61.5), anti-TCRβ (H57–597), anti-Gr-1 (RB6–8C5), and anti-TER119; phycoerythrin (PE)-Cy5-conjugated Sca-1 (D7) and isotype control rat IgG2a; and allophycocyanin (APC)-conjugated secondary anti-mouse IgG. From BD Biosciences: purified anti-polySia (12F8), anti-NCAM (NCAM-13) and rat IgM isotype control; fluorescein-conjugated anti-CD8a (53-6.7) anti-TCRγδ (GL3), anti-NK1.1 (PK136), anti-B220 (RA3–6B2) and isotype controls mouse IgG2a (G155–178), rat IgG1 (R3–34), rat IgG2a (R35–95), and rat IgG2b (A95-1); PE-conjugated anti-CD8a (53-6.7), anti-CD3 (SK7), anti-CD33 (Leu-M9), anti-CD81 (JS-81), anti-CD117 (104D2), anti-CD25 (PC61), and anti-CD117 (2B8) and isotype controls rat IgG1 (R3–34), and rat IgG2a (R35–95); PE-Cy5-conjugated anti-CD3 (17A2), anti-CD44 (IM7). From Jackson ImmunoResearch (West Grove, PA): APC-conjugated secondary anti-Rat IgM. From Invitrogen (Carlsbad, CA): fluorescein-conjugated anti-CD3 (S4.1), anti-CD15 (V1MC6), anti-CD34 (581) and isotype control mouse

IgM; PE-conjugated anti-CD7(CD7-6B7), anti-CD34 (581), anti-CD45 (HI30) anti-CD105 (SN6), and isotype controls mouse IgG1, mouse IgG2a and mouse IgG2b. From Beckman-Coulter (Fullerton, CA): PE-conjugated anti-CD2 (SFCI3Pt2H9-T11). From Exalpha Corporation (Boston, MA): fluorescein-conjugated anti-CD56 (C5.9). The production of mAb 735 has been described (18).

Flow cytometry and sorting

Cells were isolated and immediately incubated for 10 min with Mouse BD Fc Block (anti-FcγIII/II R; BD Biosciences), followed by the addition of antibodies for staining. After 20 min cells were washed twice in PBS and analyzed on a FACSCalibur (BD Biosciences) using CellQuest (BD Biosciences) software. Hematopoietic stem cells were defined as Lin- (including TER119, CD3, CD4, CD8, B220, NK1.1, Gr-1, TCRβ, TCRγδ, CD11b), cKit+, Sca-1+. Human cells were analyzed on an LSR II flow cytometer (BD Biosciences). Meta-analyses were performed using FlowJo software (Tree Star, Inc.; Ashland, OR). Differences between controls, which were stained with a irrelevant antibody of the same isotype, and the experimentals, which expressed polySia, were calculated using the population comparison function of FlowJo software. For sorted cells, freshly isolated mouse bone marrow was centrifuged over a layer of Ficoll-Paque Plus (Amersham Biosciences; Little Chalfont, Buckinghamshire, UK), then light-density cells were labeled with anti-cKit (PE) and purified anti-polySia (12F8) followed by anti-Rat IgM (APC). Desired cell subsets were sorted using a DAKO-Cytomation MoFlo High Speed Sorter (Dako; Glostrup, Denmark) or a FACSAria (BD Biosciences).

Colony-forming cell (CFC) assays

Erythroid progenitor cultures were initiated in septuplicate with 2.5×10^2 to 2.0×10^3 cells/dish. CFC assays were performed as previously described (19) in serum-deprived medium with substitution of 10% FBS for low-density lipoprotein (HyClone Laboratories, Logan, Utah). Growth was supported by 100 ng/ml recombinant rat stem cell factor (rrSCF, Amgen, Inc., Thousand Oaks, CA), and 10 units/ml recombinant human (rh) erythropoietin (EPO, Amgen Inc.). After 7 days, cultures were scored for burst-forming units erythroid (BFU-E) identified as distinct clusters of erythroid ± myeloid cells and myeloid CFC having a dispersed cell morphology. Myeloid progenitors were assayed as previously described (20). Sorted cells were cultured, in triplicate, at 1.0×10^2 to 2.0×10^3 cells/dish in the described medium containing 100 ng/ml rrSCF, 20 ng/ml rh interleukin (IL)-6, 20 ng/ml recombinant murine IL-3, 20 ng/ml rh macrophage colony-stimulating factor (M-CSF, R&D Systems, Minneapolis, MN), and 20 ng/ml rh granulocyte colony-stimulating factor (G-CSF, Amgen, Inc.). After 7 days, cultures were scored visually for colonies (50+ cells) and clusters (10–49 cells). The erythroid and myeloid assays were repeated twice with similar results.

Lymphoid Progenitor Assay

OP9 cells transfected with Delta-like-1 (DL1) and GFP, or with GFP alone were kindly provided by Dr. Juan Carlos Zúñiga-Pflücker (Sunnybrook & Women's Research Institute). OP9-GFP and OP9-DL1 cells were cultured and passaged as described (21). Sorted bone marrow subsets were plated onto a semi-confluent layer of either OP9-GFP or OP9-DL1 cells in Complete DMEM-10 with 1 ng/mL IL-7 (R&D Systems; Minneapolis, MN) and 5 ng/ml Flt-3 ligand (R&D Systems). Co-cultures were maintained, passaged as described (21) and harvested at 18 d. Cells were counted with a hemocytometer and analyzed by flow cytometry for expression of lineage markers. The experiment was repeated three times with similar results.

5-Fluorouracil (5-FU) Recovery

Wild-type mice (6–8 wk) received a single intraperitoneal dose of either 5-FU (150 mg/kg) or vehicle. Following drug administration, bone marrow was harvested from 2 to 3 mice at each timepoint (days 1, 2, 7, 10 and 12) for flow cytometric analyses. The experiment was repeated three times with similar results.

G-CSF Response

Wild-type mice (6–8 wk) were injected intraperitoneally once a day for 5 d with 100 μl of either vehicle (PBS + 2% bovine serum albumin) or vehicle containing 2 μg G-CSF. Mice, 2 to 3 per group, were sacrificed after 5 d. Bone marrow was harvested for analysis by flow cytometry. The experiment was repeated three times with similar results.

Immunoblotting

Freshly isolated mouse bone marrow and brain samples were disrupted on ice in 20 mM Tris-Cl, pH 8.0, 140 mM NaCl, 10% glycerol, 1% NP-40, 2 mM EDTA, 10 mM NaF and proteinase inhibitor cocktail (Calbiochem; La Jolla, CA). Lysates were separated on a 3–8% Tris-acetate gel (BioRad; Hercules, CA), transferred to nitrocellulose (BioRad) and non-specific reactivity was blocked by incubating the blots for 2 h in 5% milk in PBS with 0.05% Tween-20 (PBST). Blots were then incubated overnight at 4 °C in PBST with primary antibody at 1:5000 (anti-polySia, mAb 735) or 1:500 (anti-NCAM, mAb NCAM-13). After washing 3 × 5 min in PBST, blots were incubated for 90 min at room temperature in PBST with horseradish peroxidase-conjugated secondary antibodies (Jackson ImmunoResearch) at 1:5000. Blots were washed 3 × 5 min in PBST and signal was detected using Super Signal West Pico Chemiluminescence Substrate (Pierce, Rockford, IL).

Immunoprecipitation

Bone marrow lysates were prepared as described above from 10 wild-type and 10 ST8Sia IV-/- mice, and pre-cleared by a 30 min incubation at 4 °C with Protein G-Sepharose beads (Invitrogen). Antibody-conjugated beads were prepared by incubating 5 μg mAb 735 with 50 μl Protein G-Sepharose beads at 4 °C. mAb 735-conjugated beads were added to lysates and tumbled for 1 h at 4 °C. Following incubation, beads were washed extensively in ice-cold wash buffer [0.1% Triton X-100, 50 mM Tris-Cl, pH 7.4, 300 mM NaCl, 5 mM EDTA, 0.02% NaN_3 (w/v)], and then in ice-cold PBS. PolySia was removed from captured proteins by direct treatment with 2 μl of Endo N (3 h at 37 °C). Then the sample was boiled in sample buffer (XT Sample buffer, XT Reducing agent; BioRad) and run on a 3–8% Tris-acetate gel (BioRad). Bands were visualized with a mass spectrometry-compatible silver stain (Silver Quest; Invitrogen).

Protein digestion and identification by mass spectrometry

The preparation and analysis of samples was performed at the Taplin Biological Mass Spectrometry Facility, Harvard Medical School. Silver-stained bands were excised and digested with trypsin, and analyzed by ESI-LC-MS/MS on an LTQ linear ion-trap mass spectrometer (ThermoFisher, San Jose, CA). Peptide sequences (and hence protein identity) were determined by matching protein databases with the acquired fragmentation pattern by the software program, Sequest (ThermoFisher) (22). Spectral matches were manually examined and multiple identified peptides per protein were required.

In vivo progenitor assay

ST8Sia IV-/- mice were crossed with congenic wild-type mice expressing GFP (Stock # 004353, The Jackson Laboratory). F1 progeny were back-crossed with ST8Sia IV-/- animals

to yield ST8Sia IV-/-; GFP+/- mice, which were used as bone marrow donors for these studies. Genotype was confirmed by PCR as previously described (14). Sorted cell populations were mixed with 1×10^6 whole wild-type bone marrow cells for injection. Wild-type recipient mice (3 per donor subset) were irradiated with one dose of 900 rad, and injected intravenously with prepared cells. After 21 d, recipients were sacrificed and their lymphoid organs analyzed for GFP+ cells. The experiment was repeated twice with similar results.

Contact hypersensitivity (CHS)

2,4-Dinitrofluorobenzene (DNFB) was used to induce CHS in wild-type or ST8Sia IV-/- mice, 3–10 mice per group. Animals were sensitized by painting bare abdominal skin on two consecutive days with 20 μl of 0.5% DNFB in acetone:olive oil (4:1). Mice were challenged 7 d later with an application of 20 μl of 0.5% DNFB on the right ear, and vehicle alone on the left ear. The inflammatory response was assessed by measuring ear thickness with digital calipers at 24 h, 48 h and 72 h. In some cases, animals were euthanized and their ears removed for histological evaluation. The experiment was repeated four times with similar results.

Tumor challenge

Mouse RMA and RMA-S (which have reduced MHC class I expression) NK-T cell tumor cell lines were obtained from the American Type Culture Collection (Manassas, VA). Each experimental group (wild-type and ST8Sia IV-/-) contained 5–10 mice (4–12 wks) that were age matched within 2 wks. RMA or RMA-S cells (10^4 to 10^5) were injected subcutaneously into the flank. Palpable tumors were measured daily with digital calipers. Mice were euthanized after loss of > 20% of original body weight, when a tumor reached >1.5 cm or became ulcerated. Animals surviving 60 d were considered tumor-free. The experiment was repeated twice with similar results.

Hematology and histology

The UC Davis Comparative Pathology Laboratory performed complete blood counts, which were validated by visual examination of blood smears. Histological evaluation of CHS ear specimens was also performed.

Statistics

Unless otherwise stated, numbers represent the mean ± one standard deviation (SD). Statistical significance in tumor assays was calculated using a two-tailed Mann-Whitney test. Statistical significance of the remaining data was calculated using an unpaired two-tailed Student's t-test. $p < 0.05$ was considered significant.

Results

Human NK cells modulate NCAM protein expression and degree of polysialylation with activation state

Flow cytometric analyses showed that human PBMCs expressed the NCAM protein scaffold and its polysialic acid modifications, which were sensitive to the polySia-specific neuraminidase Endo N (Fig. 1A). Upon activation with IL-2, the cell-surface levels of both the underlying protein and the attached glycan increased (Fig. 1B; n = 10). To address whether the observed increase in polySia expression reflected differential proliferation of $CD56^{dim}$ and $CD56^{bright}$ NK cell populations during the assay, sorted cells with these phenotypic characteristics were analyzed in parallel; similar responses were observed (data not shown). These data suggest that polySia levels are regulated by NK cell activation.

As the DP of polySia on human primary cells has not been explored, purified NK cells were cultured with or without IL-2 for 48 hours. Samples from five individual donors were combined for analysis. Intact polySia chains on glycan cores containing lactosamine were released by Endo-β-galactosidase treatment. This method may have neglected to free polySia that was attached to NCAM through alternate core structures, however the relative amounts of total sialic acid released from resting and activated NK cells was in accord with our flow cytometry (Fig. 1) and immunoblotting data (not shown). The liberated polySia was analyzed by high-performance liquid chromatography (HPLC) as previously described to determine chain length (2). Total sialic acid content [as *N*-acetyl neuraminic acid (NANA)] of HPLC fractions was monitored to track the relative abundance of each DP population. In both resting and activated NK cells, a large fraction of total NANA was associated with small non-polySia glycans (DP 1–10), most likely reflecting the capping groups of typical N- and O-linked glycans. Plotting percent of total NANA versus DP showed that activation of NK cells increased the abundance of NANA associated with polySia (Fig. 2). Additionally, chain length, which was extremely heterogeneous on resting cells, was compressed into the mid-range (DP 11–140) upon activation.

ST8Sia IV catalyzes polySia expression by populations of mouse bone marrow cells during myeloid differentiation

To analyze the potential immunological properties of polySia, we used a mouse model. First, we characterized the expression patterns of polySia on immune subsets in wild-type animals. In contrast to their human counterparts, polySia was not detectable on mouse NK cells (Fig. 3C). This finding was consistent with RT-PCR analyses on sorted NK cells that revealed an absence of NCAM and ST8Sia IV (data not shown). Interestingly, robust polySia expression was detected on wild-type mouse bone marrow subsets (Fig. 3A). This expression was conserved in ST8Sia II-/- but absent in ST8Sia IV-/- mice, indicating that the latter enzyme was responsible for polySia on these cells.

Bone marrow polySia expression correlated with receptor tyrosine kinase cKit expression, suggesting that the polySia+ cells were hematopoietic progenitors. We defined four subsets according to their relative levels of polySia (PSA) and cKit (Kit) (PSA^{neg}/Kit^{hi}, PSA^{lo}/Kit^{hi}, PSA^{hi}/Kit^{hi}, PSA^{lo}/Kit^{lo}; Fig. 3A). The populations comprised 12%, 6%, 12% and 42%, respectively, of total cKit+ bone marrow cells. Extensive phenotypic analyses by flow cytometry suggested that these subsets comprised cells that were differentiating along a myeloid pathway (Table I). The PSA^{neg}/Kit^{hi} population included hematopoietic stem cells (HSCs) (defined as Lin-, cKit+, Sca-1+) and the majority appeared to be progenitors as they were Lin- and expressed CD34. The second population (PSA^{lo}/Kit^{hi}) comprised more committed progenitors with near uniform expression of CD34, and to a lesser extent CD11b and Gr-1. As differentiation proceeded, evidenced by a reduction in CD34 expression and an increase in CD11b and Gr-1 expression, PSA levels dramatically increased in parallel (PSA^{hi}/Kit^{hi}). The fully differentiated progeny, (CD34+/-, CD11b+, $Gr\text{-}1^{hi}$) had polySia levels that were comparable to the progenitors (PSA^{lo}/Kit^{lo}). Consistent with the latter population containing mature myeloid cells, we found low levels of polySia expression on peripheral wild-type, but not ST8Sia IV-/-, Gr-1+ splenocytes (Fig. 3B). Thus, myeloid differentiation is characterized by a wave of high levels of polySia expression. In contrast to the mouse, human fetal bone marrow did not contain these polySia+ myeloid populations, and human peripheral myeloid cells did not express polySia (data not shown). The polySia+ subset in human fetal bone marrow consisted of NK cells, as determined by the phenotype: CD56+, CD7+, CD33- and CD34- (data not shown). It is worth noting that the observed differences between adult mouse bone marrow and fetal human bone marrow may be attributable to variations in polySia expression during development.

In vitro progenitor studies confirm the phenotypic analyses of the polySia expressing subsets

To confirm the phenotypic analyses, the bone marrow populations defined by polySia and cKit were sorted by flow cytometry and tested in vitro and in vivo for their ability to give rise to various immune lineages. For these experiments, the PSA^{neg}/Kit^{hi} subset served as a positive control, as hematopoietic stem cells were contained in this population (data not shown). In colony-forming assays testing erythroid and myeloid potential, both the positive control and the progenitor subset, PSA^{lo}/Kit^{hi}, gave rise to these lineages, forming both erythroid blasts and colonies, and myeloid colonies and clusters (Fig. 4A and B). Of the more differentiated populations, the immature myeloid cells, PSA^{hi}/Kit^{hi}, showed an intermediate ability to form myeloid clusters, and did not produce erythroid populations. The fully differentiated PSA^{lo}/Kit^{lo} cells did not produce colonies in either assay.

To test lymphoid progenitor potential, sorted bone marrow subsets were co-cultured with OP9 cells transfected with a GFP vector control, or with GFP and the Notch ligand, Delta-like 1 (DL1). In this assay, multipotent progenitors develop into B cells when cultured on OP9-GFP feeders, while DL1 induces T-cell development. NK cells develop at lower efficiencies under both conditions. In accord with the phenotypic data and colony-forming assays, the positive control, PSA^{neg}/Kit^{hi}, and the progenitor population, PSA^{lo}/Kit^{hi}, produced all the lymphoid lineages, the latter with a 10-fold reduction in efficiency as compared to the former (Fig. 5). The immature myeloid subset, PSA^{hi}/Kit^{hi}, did not produce NK or T cells, and generated almost 1000-fold fewer B cells than the positive control population. The mature myeloid population, PSA^{lo}/Kit^{lo}, did not proliferate.

In vivo progenitor studies confirm the phenotypic and in vitro analyses of the polySia expressing subsets

For in vivo experiments, GFP+ congenic wild-type mice were used as donors so that engrafted lineages could be identified using this fluorescent reporter. Flow-sorted bone marrow subsets (~28,000 cells/mouse) were injected with a survival dose (1×10^6 cells/mouse) of wild-type bone marrow into irradiated wild-type recipient animals. Three weeks later mice were sacrificed and organs analyzed for GFP+ populations (Table II). Both the positive control, PSA^{neg}/Kit^{hi}, and the progenitor population, PSA^{lo}/Kit^{hi}, gave rise to erythroid (TER119+), myeloid (Gr-1+ and CD14+) and lymphoid (DX5+ and B220+) cells in the bone marrow and spleen. No statistically significant differences were noted in the numbers of cells recovered from these two donor populations. In contrast, the numbers of GFP+ cells isolated from the immature myeloid subset, PSA^{hi}/Kit^{hi}, and the mature myeloid population, PSA^{lo}/Kit^{lo}, were reduced by an average of ~ 40-fold and ~ 500-fold, respectively, as compared to the progenitor subsets.

Next, we asked whether development of the four bone marrow subsets was temporally linked. Mice were treated with one bolus of 5-fluorouracil to deplete cycling cells, and the disappearance and reappearance of the polySia/cKit-defined populations was followed over 12 days. As expected, the depletion and recovery of the progenitors preceded by one to two days that of the mature subsets (Fig. 6).

Finally, we stimulated myeloid development and characterized the response of the bone marrow subsets. Briefly, wild-type mice were injected every 24 hours with granulocyte-colony stimulating factor (G-CSF) for five days to induce expansion of the myeloid compartment, and bone marrow was analyzed by flow cytometry. In accord with the preceding phenotypic, in vitro and in vivo data, both the progenitor population, PSA^{lo}/Kit^{hi} and the immature and mature myeloid subsets (PSA^{hi}/Kit^{hi} and PSA^{lo}/Kit^{lo}) significantly expanded in response to G-CSF treatment as compared to vehicle-treated control mice ($p < 0.01$; Fig. 7). Collectively, the data

in Table II and Fig. 3–Fig. 7 reveal that polySia expression is expressed and modulated during myeloid development in the mouse.

Given the expression of polySia on hematopoietic progenitors and myeloid cells, we asked whether there were obvious changes in the distribution of immune subsets in ST8Sia IV-/- as compared to wild-type mice. Hematological analyses revealed minimal differences—a statistically significant, slight increase in the percentage of lymphocytes in peripheral blood and a corresponding though not significant decrease in the percentage of circulating monocytes and neutrophils (data not shown). No changes in the numbers or phenotype of peripheral myeloid lineages were noted (data not shown).

NCAM is the scaffold for myeloid expression of polySia

As this study was the first description of polySia on myeloid cells, the underlying protein scaffold was unknown. Candidate proteins that are expressed by other cell types that carry polySia modifications include NCAM and CD36. To identify the scaffold on the myeloid subsets that were the subject of this investigation, we immunoprecipitated wild-type and ST8Sia IV-/- bone marrow lysates with an anti-polySia antibody, treated the precipitatate with Endo N to remove polySia, and separated the deglycosylated proteins by SDS-PAGE. Following electrophoresis, two silver stained bands of approximately 120 and 140 kDa were observed in the wild-type, but not the ST8Sia IV-/- samples (Fig. 8A). The bands were excised and analyzed by electrospray mass spectrometry (LTQ linear ion trap), which identified both bands, on the basis of two peptides each, as NCAM (data not shown). In accord with this finding, both flow cytometry and immunoblotting confirmed the presence of NCAM on the relevant cells in mouse bone marrow (Fig. 8B and C).

ST8Sia IV-/- mice exhibit exaggerated contact hypersensitivity and an inability to control growth of engrafted tumors

Next we tested immune responses in ST8Sia IV-/- mice. First, we used a contact hypersensitivity (CHS) assay. Wild-type and ST8Sia IV-/- mice were sensitized with the hapten dinitrofluorobenzene (DNFB); a week later, they were challenged with an application of DNFB to one ear, and vehicle alone to the other ear. Wild-type mice responded as expected, with peak swelling observed around 24 hours (23). Interestingly, the ST8Sia IV-/- response equaled or exceeded the wild-type response at 24 hours, and inflammation continued to increase through 48 and 72 hours. Fig. 9A shows the results of a representative experiment in which ST8Sia IV-/- ear thickness was statistically increased at all timepoints as compared to the response of wild-type animals.

We also assessed the CHS response at 72 hours on a histological level, and noted significantly more inflammation and edema after DNFB treatment of ST8Sia IV-/- mice as compared to controls, whose lesions were much less severe (Fig. 9B). Injury to the epithelium of ST8Sia IV-/- ears was also more pronounced, with diffuse epidermal hyperplasia, intercellular edema and ulceration. The ST8Sia IV-/- vehicle-treated ears also demonstrated minimal to mild edema whereas the wild-type controls had no significant lesions.

We used immunosensitive and immunoresistant cell lines to test the response of ST8Sia IV-/- mice to a tumor challenge. RMA-S cells, which have reduced MHC class I expression, are sensitive to NK killing, while the parental RMA cells form tumors in wild-type animals (24). In initial experiments, RMA-S cells formed tumor masses in NK-cell-depleted wild-type animals (25), but not wild-type or ST8Sia IV-/- mice. This finding suggested that the NK-cell compartment of ST8Sia IV-/- mice was intact (data not shown). In contrast, injection of RMA cells into wild-type, ST8Sia IV-/- or the immunodeficient TCRβ-/- mice led to uncontrolled tumor growth in all cohorts, requiring euthanasia of the animals when their tumors exceeded

acceptable size limitations (Fig. 10). Importantly, tumor growth in ST8Sia IV-/- mice was significantly faster than in wild-type mice, and was comparable to the rate observed in TCRβ-/- mice ($p < 0.02$).

Discussion

PolySia expression and function has been extensively studied in the nervous system, but its distribution and role in the immune compartment is still undefined. Here we demonstrated the presence of polySia on human NK cells, and its absence on other immune subsets, a finding that is in accord with two earlier reports (26,27). NK cells upregulated the expression of polySia and its scaffold NCAM upon activation by IL-2 treatment. This co-regulation suggested that the heightened polySia signals were due to an upregulation of both scaffold and glycan, rather than solely attributable to expanded polySia chain length. In support of this conclusion, a comparison of DP on resting and activated cells showed that upon activation total polySia was increased and the DP became more homogenous—tending towards small to medium length chains. To our knowledge, this is the first elucidation of polySia DP on primary human cells. The DP values we observed were slightly larger than analogous structures that were isolated from cell lines and chick brain (1,28). Although this distinction may be due to real differences among samples, it more likely reflects the fact that our method protects samples from acid-catalyzed internal hydrolysis. Importantly, this result shows that the size of polySia chains on human immune cells is comparable to that of glycosaminoglycans (GAGs), polysaccharides that play critical structural and functional roles in the extracellular matrix compartment. The repeating negative charge present on polySia is also reminiscent of highly anionic GAGs, and this characteristic is likely critical to its function.

Mouse NK cells did not express NCAM or polySia; however, both were co-expressed in mouse bone marrow. Immunoprecipitation of bone marrow lysates with anti-polySia antibodies and identification of the resulting bands by mass spectrometry demonstrated that NCAM was the underlying scaffold. Analyses of ST8Sia II-/- and ST8Sia IV-/- mice indicated that the latter enzyme produced the glycan.

Flow cytometry revealed four bone marrow subsets based on expression of polySia and cKit. These populations (PSA^{neg}/Kit^{hi}, PSA^{lo}/Kit^{hi}, PSA^{hi}/Kit^{hi}, PSA^{lo}/Kit^{lo}) bore cell surface antigens that were characteristic of myeloid differentiation. The PSA^{neg}/Kit^{hi} subset contained hematopoeitic progenitors, the PSA^{lo}/Kit^{hi} population, multipotent progenitors, and the PSA^{hi}/Kit^{hi}, PSA^{lo}/Kit^{lo} groups, immature and mature myeloid cells, respectively. These findings were confirmed by in vitro and in vivo functional studies. 5-FU experiments demonstrated that the developmental kinetics of the four populations were temporally linked, and thus these populations shared a common lineage. Finally, the progenitor population, PSA^{lo}/Kit^{hi}, and the immature and mature myeloid subsets, PSA^{hi}/Kit^{hi} and PSA^{lo}/Kit^{lo}, respectively, all expanded in response to treatment with G-CSF, further evidence that these populations are myeloid.

We observed a dramatic different in CHS response in ST8Sia IV-/-, which sustained augmented inflammation, as compared to wild-type. This striking observation elicits some interesting hypotheses. Considering possible roles for polySia in the immune system, we noted that both NK and myeloid cells are cytotoxic populations, carrying small positively-charged anti-microbial peptides (AMPs) (29–31). Negatively-charged GAGs such as heparan sulfate can bind and neutralize AMPs, (32,33) thus it is possible that polySia with its structural similarities to GAGs, has parallel activities. Expression of polySia on cytotoxic cells may localize AMPs released from leukocytes to prevent damage of surrounding tissues. The excessive CHS inflammatory response noted in ST8Sia IV-/- mice is consistent with this notion, as granulocytes that were initially drawn to the site might have injured tissues by uncontrolled

AMP leakage. In turn, damaged tissue would release proinflammatory signals, upregulating the immune response (34). This cycle is consistent with the protracted inflammatory reaction, the increased tissue damage, and the elevated leukocytic infiltrate noted in ST8Sia IV-/- DNFB-treated ears relative to wild-type.

Additionally, GAGs, which bind cytokines and chemokines, modulate their availability and local concentration by either presenting or sequestering these molecules. It is possible that polySia plays a similar role. Studies in the nervous system have already demonstrated that neuronal responses to the cytokines brain-derived neurotrophic factor (BDNF) and platelet-derived growth factor (PDGF) are affected by polySia expression, although the mechanism has not been elucidated (9,10). As the development and function of the immune system depends heavily on the influence of cytokines, polySia could have a great impact. However, its effects would likely be complex since cytokines that regulate signaling networks that, in turn, direct fate decisions, trafficking and activation might be involved. The decreased immune response to ectopic tumors noted in ST8Sia IV-/- mice raises the intriguing possibility that these processes are influenced by polySia.

To our knowledge, this is the first demonstration of either polySia or NCAM expression on myeloid cells. The discovery of such expression in the mouse provides an opportunity to manipulate and study the immunological role of these molecules in a biological context, including in vivo models. The findings could have important implications for human health, as polySia and NCAM are not only expressed on human NK cells but also decorate the surfaces of a variety of tumors and bacteria. For instance, polysialylated NCAM, which is found on a number of cancers including gliomas, small cell lung carcinomas and Wilms' tumors, is positively associated with metastasis and disease progression (35–37). We postulate that tumors co-opt the immune system's strategy of using polySia to modulate responses to chemokines and growth factors, thus gaining a competitive advantage. Regarding bacteria, polySia expression is correlated with the virulence of pathogenic strains of *E. coli* K1 and Group B *N. meningitides* (38,39). It is possible that bacterial polySia binds and neutralizes AMPs, sequestering them at a safe distance from the cell wall. Similarly, a subset of chemokines also has antibiotic activity (40), and polySia, which has been shown to modulate chemokine functions (9,10), may protect bacteria from this threat. Collectively, our data point to a role for polySia in the complex processes involved in immunological development and host defense.

References

1. Inoue S, Inoue Y. Developmental profile of neural cell adhesion molecule glycoforms with a varying degree of polymerization of polysialic acid chains. J Biol Chem 2001;276:31863–31870. [PubMed: 11371567]
2. Nakata D, Troy FA 2nd. Degree of polymerization (DP) of polysialic acid (polySia) on neural cell adhesion molecules (N-CAMS): development and application of a new strategy to accurately determine the DP of polySia chains on N-CAMS. J Biol Chem 2005;280:38305–38316. [PubMed: 16172115]
3. Varki, A.; Cummings, R.; Esko, J.; Freeze, H.; Hart, G.; Marth, J. Essentials of Glycobiology. Cold Spring Harbor, NY: Cold Spring Harbor Laboratory Press; 1999.
4. Curreli S, Arany Z, Gerardy-Schahn R, Mann D, Stamatos NM. Polysialylated neuropilin-2 is expressed on the surface of human dendritic cells and modulates dendritic cell-T lymphocyte interactions. J Biol Chem 2007;282:30346–30356. [PubMed: 17699524]
5. von Der Ohe M, Wheeler SF, Wuhrer M, Harvey DJ, Liedtke S, Muhlenhoff M, Gerardy-Schahn R, Geyer H, Dwek RA, Geyer R, Wing DR, Schachner M. Localization and characterization of polysialic acid-containing N-linked glycans from bovine NCAM. Glycobiology 2002;12:47–63. [PubMed: 11825886]

6. Yabe U, Sato C, Matsuda T, Kitajima K. Polysialic acid in human milk. CD36 is a new member of mammalian polysialic acid-containing glycoprotein. J Biol Chem 2003;278:13875–13880. [PubMed: 12576469]
7. Zuber C, Lackie PM, Catterall WA, Roth J. Polysialic acid is associated with sodium channels and the neural cell adhesion molecule N-CAM in adult rat brain. J Biol Chem 1992;267:9965–9971. [PubMed: 1315775]
8. Murakami S, Seki T, Rutishauser U, Arai Y. Enzymatic removal of polysialic acid from neural cell adhesion molecule perturbs the migration route of luteinizing hormone-releasing hormone neurons in the developing chick forebrain. J Comp Neurol 2000;420:171–181. [PubMed: 10753305]
9. Zhang H, Vutskits L, Calaora V, Durbec P, Kiss JZ. A role for the polysialic acid-neural cell adhesion molecule in PDGF-induced chemotaxis of oligodendrocyte precursor cells. J Cell Sci 2004;117:93–103. [PubMed: 14627627]
10. Vutskits L, Djebbara-Hannas Z, Zhang H, Paccaud JP, Durbec P, Rougon G, Muller D, Kiss JZ. PSA-NCAM modulates BDNF-dependent survival and differentiation of cortial neurons. Eur J Neurosci 2001;13:1391–1402. [PubMed: 11298800]
11. Petridis AK, El-Maarouf A, Rutishauser U. Polysialic acid regulates cell contact-dependent neuronal differentiation of progenitor cells from the subventricular zone. Dev Dyn 2004;230:675–684. [PubMed: 15254902]
12. Angata K, Nakayama J, Fredette B, Chong K, Ranscht B, Fukuda M. Human STX polysialyltransferase forms the embryonic form of the neural cell adhesion molecule. Tissue-specific expression, neurite outgrowth, and chromosomal localization in comparison with another polysialyltransferase, PST. J Biol Chem 1997;272:7182–7190. [PubMed: 9054414]
13. Lanier LL, Testi R, Bindl J, Phillips JH. Identity of Leu-19 (CD56) leukocyte differentiation antigen and neural cell adhesion molecule. J Exp Med 1989;169:2233–2238. [PubMed: 2471777]
14. Eckhardt M, Bukalo O, Chazal G, Wang L, Goridis C, Schachner M, Gerardy-Schahn R, Cremer H, Dityatev A. Mice deficient in the polysialyltransferase ST8SiaIV/PST-1 allow discrimination of the roles of neural cell adhesion molecule protein and polysialic acid in neural development and synaptic plasticity. J Neurosci 2000;20:5234–5244. [PubMed: 10884307]
15. Angata K, Long JM, Bukalo O, Lee W, Dityatev A, Wynshaw-Boris A, Schachner M, Fukuda M, Marth JD. Sialyltransferase ST8Sia-II assembles a subset of polysialic acid that directs hippocampal axonal targeting and promotes fear behavior. J Biol Chem 2004;279:32603–32613. [PubMed: 15140899]
16. Drake PM, Gunn MD, Charo IF, Tsou CL, Zhou Y, Huang L, Fisher SJ. Human placental cytotrophoblasts attract monocytes and CD56(bright) natural killer cells via the actions of monocyte inflammatory protein 1alpha. J Exp Med 2001;193:1199–1212. [PubMed: 11369791]
17. Golfier F, Barcena A, Harrison MR, Muench MO. Fetal bone marrow as a source of stem cells for in utero or postnatal transplantation. Br J Haematol 2000;109:173–181. [PubMed: 10848797]
18. Frosch M, Gorgen I, Boulnois GJ, Timmis KN, Bitter-Suermann D. NZB mouse system for production of monoclonal antibodies to weak bacterial antigens: isolation of an IgG antibody to the polysaccharide capsules of Escherichia coli K1 and group B meningococci. Proc Natl Acad Sci U S A 1985;82:1194–1198. [PubMed: 3919387]
19. Muench MO, Namikawa R. Disparate regulation of human fetal erythropoiesis by the microenvironments of the liver and bone marrow. Blood Cells Mol Dis 2001;27:377–390. [PubMed: 11259159]
20. Muench MO, Schneider JG, Moore MA. Interactions among colony-stimulating factors, IL-1 beta, IL-6, and kit-ligand in the regulation of primitive murine hematopoietic cells. Exp Hematol 1992;20:339–349. [PubMed: 1373685]
21. Ramsdell, F.; Zuniga-Pflucker, JC.; Takahama, Y. In Vitro Systems for the Study of T Cell Development: Fetal Thymus Organ Culture and OP9-DL1 Cell Coculture. In: Coligan, JE., editor. Current Protocols in Immunology. John Wiley & Sons, Inc; 2006. p. 3.18.11-13.18.17.
22. Eng J, McCormack AL, Yates JR 3rd. An approach to correlate tandem mass spectral data of peptides with amino acid sequences in a protein database. J Am Soc Mass Spectrom 1994;5:976–989.
23. Tuckermann JP, Kleiman A, Moriggl R, Spanbroek R, Neumann A, Illing A, Clausen BE, Stride B, Forster I, Habenicht AJ, Reichardt HM, Tronche F, Schmid W, Schutz G. Macrophages and

neutrophils are the targets for immune suppression by glucocorticoids in contact allergy. J Clin Invest 2007;117:1381–1390. [PubMed: 17446934]

24. Chen L, Sundback J, Olofsson S, Jondal M. Interference with O-glycosylation in RMA lymphoma cells leads to a reduced in vivo growth of the tumor. Int J Cancer 2006;119:1495–1500. [PubMed: 16615117]
25. Habu S, Fukui H, Shimamura K, Kasai M, Nagai Y, Okumura K, Tamaoki N. In vivo effects of anti-asialo GM1. I. Reduction of NK activity and enhancement of transplanted tumor growth in nude mice. J Immunol 1981;127:34–38. [PubMed: 7240748]
26. Husmann M, Pietsch T, Fleischer B, Weisgerber C, Bitter-Suermann D. Embryonic neural cell adhesion molecules on human natural killer cells. Eur J Immunol 1989;19:1761–1763. [PubMed: 2529126]
27. Moebius JM, Widera D, Schmitz J, Kaltschmidt C, Piechaczek C. Impact of polysialylated CD56 on natural killer cell cytotoxicity. BMC Immunol 2007;8:13. [PubMed: 17683591]
28. Poongodi GL, Suresh N, Gopinath SC, Chang T, Inoue S, Inoue Y. Dynamic change of neural cell adhesion molecule polysialylation on human neuroblastoma (IMR-32) and rat pheochromocytoma (PC-12) cells during growth and differentiation. J Biol Chem 2002;277:28200–28211. [PubMed: 12023285]
29. Chalifour A, Jeannin P, Gauchat JF, Blaecke A, Malissard M, N'Guyen T, Thieblemont N, Delneste Y. Direct bacterial protein PAMP recognition by human NK cells involves TLRs and triggers alpha-defensin production. Blood 2004;104:1778–1783. [PubMed: 15166032]
30. Kougias P, Chai H, Lin PH, Yao Q, Lumsden AB, Chen C. Defensins and cathelicidins: neutrophil peptides with roles in inflammation, hyperlipidemia and atherosclerosis. J Cell Mol Med 2005;9:3–10. [PubMed: 15784160]
31. Gallo RL, Kim KJ, Bernfield M, Kozak CA, Zanetti M, Merluzzi L, Gennaro R. Identification of CRAMP, a cathelin-related antimicrobial peptide expressed in the embryonic and adult mouse. J Biol Chem 1997;272:13088–13093. [PubMed: 9148921]
32. Jenssen H, Hamill P, Hancock RE. Peptide antimicrobial agents. Clin Microbiol Rev 2006;19:491–511. [PubMed: 16847082]
33. Malmsten M, Davoudi M, Walse B, Rydengard V, Pasupuleti M, Morgelin M, Schmidtchen A. Antimicrobial peptides derived from growth factors. Growth Factors 2007;25:60–70. [PubMed: 17454151]
34. Rock KL, Kono H. The Inflammatory Response to Cell Death. Annu Rev Pathol 2008;3:99–126. [PubMed: 18039143]
35. Bitter-Suermann D, Roth J. Monoclonal antibodies to polysialic acid reveal epitope sharing between invasive pathogenic bacteria, differentiating cells and tumor cells. Immunol Res 1987;6:225–237. [PubMed: 2448401]
36. Miyahara R, Tanaka F, Nakagawa T, Matsuoka K, Isii K, Wada H. Expression of neural cell adhesion molecules (polysialylated form of neural cell adhesion molecule and L1-cell adhesion molecule) on resected small cell lung cancer specimens: in relation to proliferation state. J Surg Oncol 2001;77:49–54. [PubMed: 11344483]
37. Suzuki M, Suzuki M, Nakayama J, Suzuki A, Angata K, Chen S, Sakai K, Hagihara K, Yamaguchi Y, Fukuda M. Polysialic acid facilitates tumor invasion by glioma cells. Glycobiology 2005;15:887–894. [PubMed: 15872150]
38. Devi SJ, Robbins JB, Schneerson R. Antibodies to poly[(2----8)-alpha-N-acetylneuraminic acid] and poly[(2----9)-alpha-N-acetylneuraminic acid] are elicited by immunization of mice with Escherichia coli K92 conjugates: potential vaccines for groups B and C meningococci and E. coli K1. Proc Natl Acad Sci U S A 1991;88:7175–7179.
39. Mushtaq N, Redpath MB, Luzio JP, Taylor PW. Prevention and cure of systemic Escherichia coli K1 infection by modification of the bacterial phenotype. Antimicrob Agents Chemother 2004;48:1503–1508. [PubMed: 15105097]
40. Yang D, Biragyn A, Kwak LW, Oppenheim JJ. Mammalian defensins in immunity: more than just microbicidal. Trends Immunol 2002;23:291–296. [PubMed: 12072367]

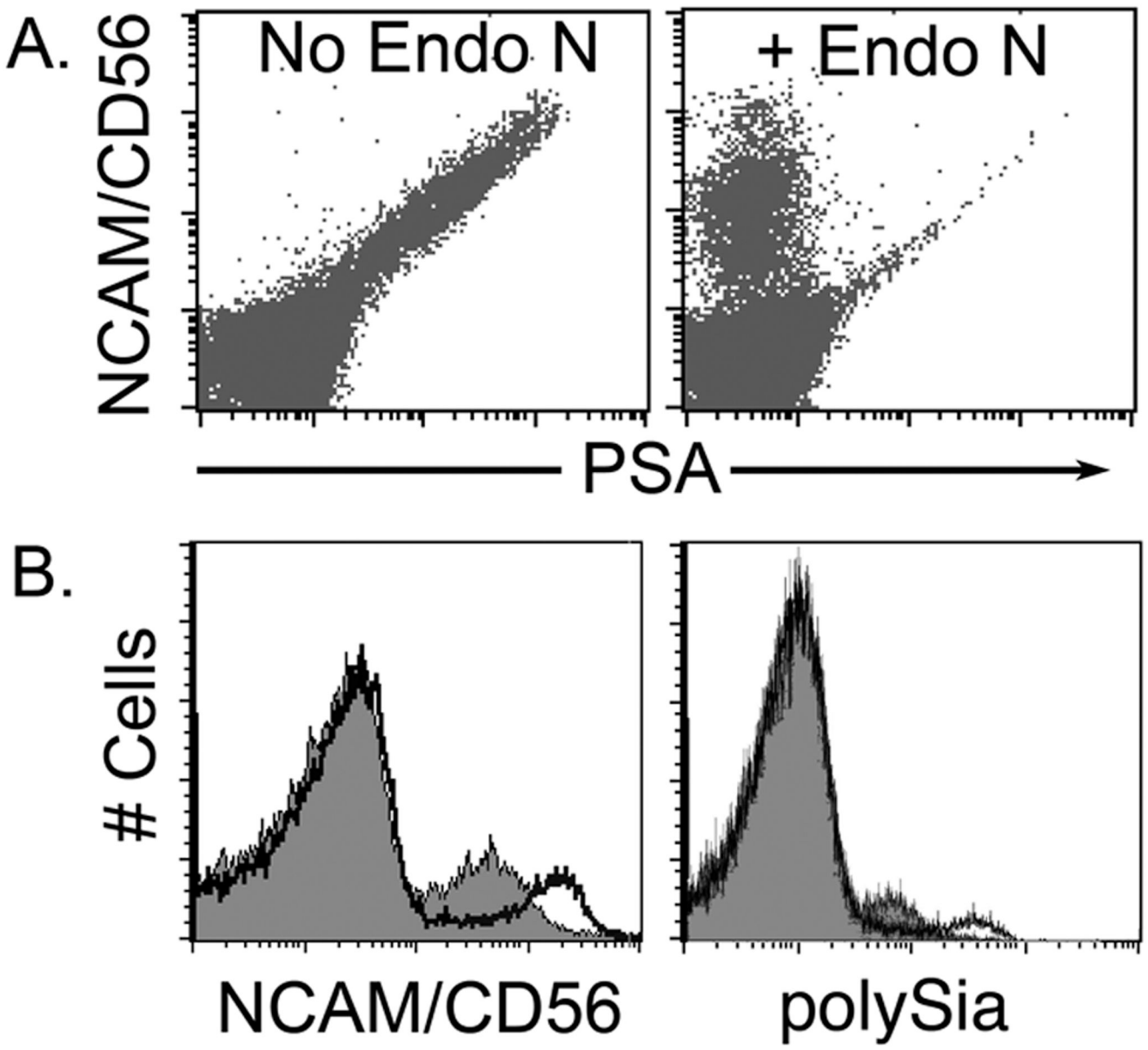

Figure 1. NCAM/CD56+ human NK cells modulate polySia and NCAM expression with activation

Flow cytometric analyses of total PBMCs after 24 h in culture with (right) or without (left) the polySia-specific neuraminidase Endo-N (A), and of total PBMCs after 48 h culture in the presence (heavy line, no fill) or absence (light line, grey fill) of IL-2 (B).

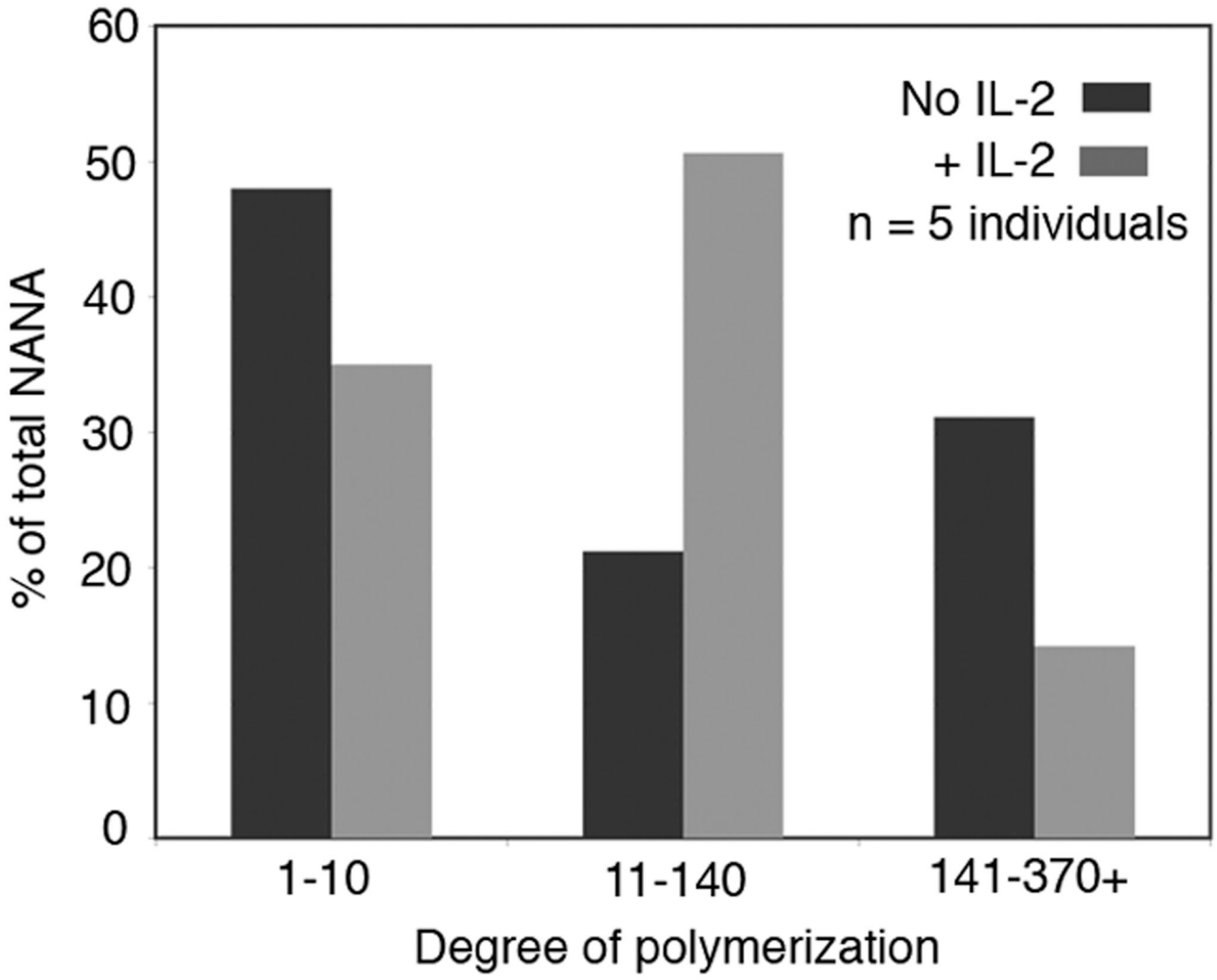

Figure 2. Human NK cell activation results in an increased production of short to medium-length polySia chains

Purified primary NK cells from five individual donors were cultured separately for 48 h with or without IL-2, combined and analyzed for DP. Fractions of increasing DP were collected (x-axis), and analyzed for total sialic acid (as NANA) content (y-axis).

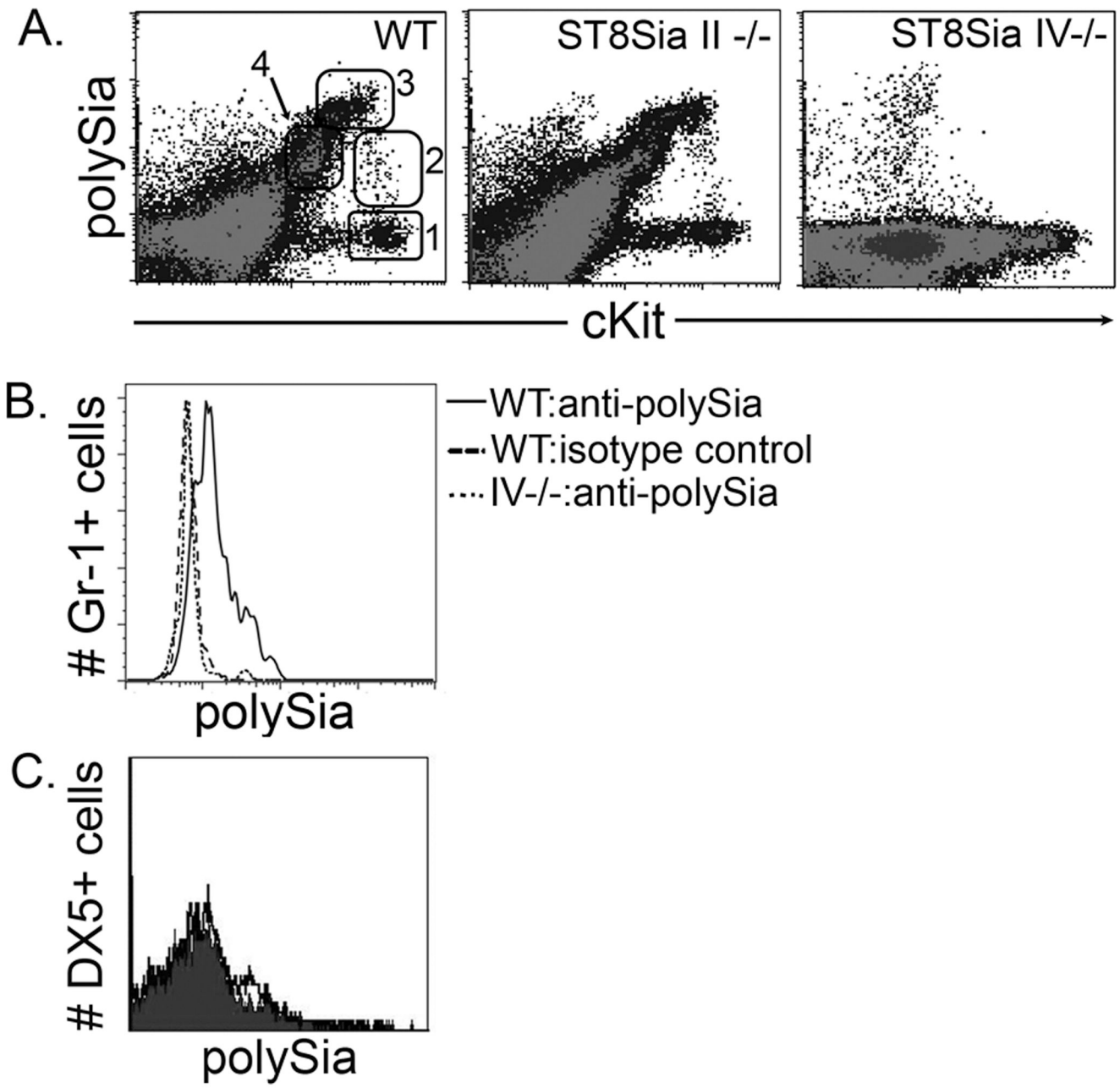

Figure 3. ST8Sia IV produces polySia on subsets of mouse bone marrow and peripheral myeloid cells

Flow cytometric analyses of total wild-type (WT) bone marrow comparing polySia and cKit expression (A). We studied four populations: PSA^{neg}/Kit^{hi} (1), PSA^{lo}/Kit^{hi} (2), PSA^{hi}/Kit^{hi} (3), and PSA^{lo}/Kit^{lo} (4). These subsets were present in ST8Sia II−/− mice, but absent from ST8Sia IV−/− animals. In the periphery (B), wild-type Gr-1+ myeloid cells expressed polySia, while the ST8Sia IV−/− cells were displayed fluorescence similar to that of the isotype control. In contrast to the human, mouse NK cells did not express polySia (C). DX5+ splenocytes were labeled with isotype control (light line, grey fill) or anti-polySia (heavy line, no fill) antibodies and analyzed by flow cytometry.

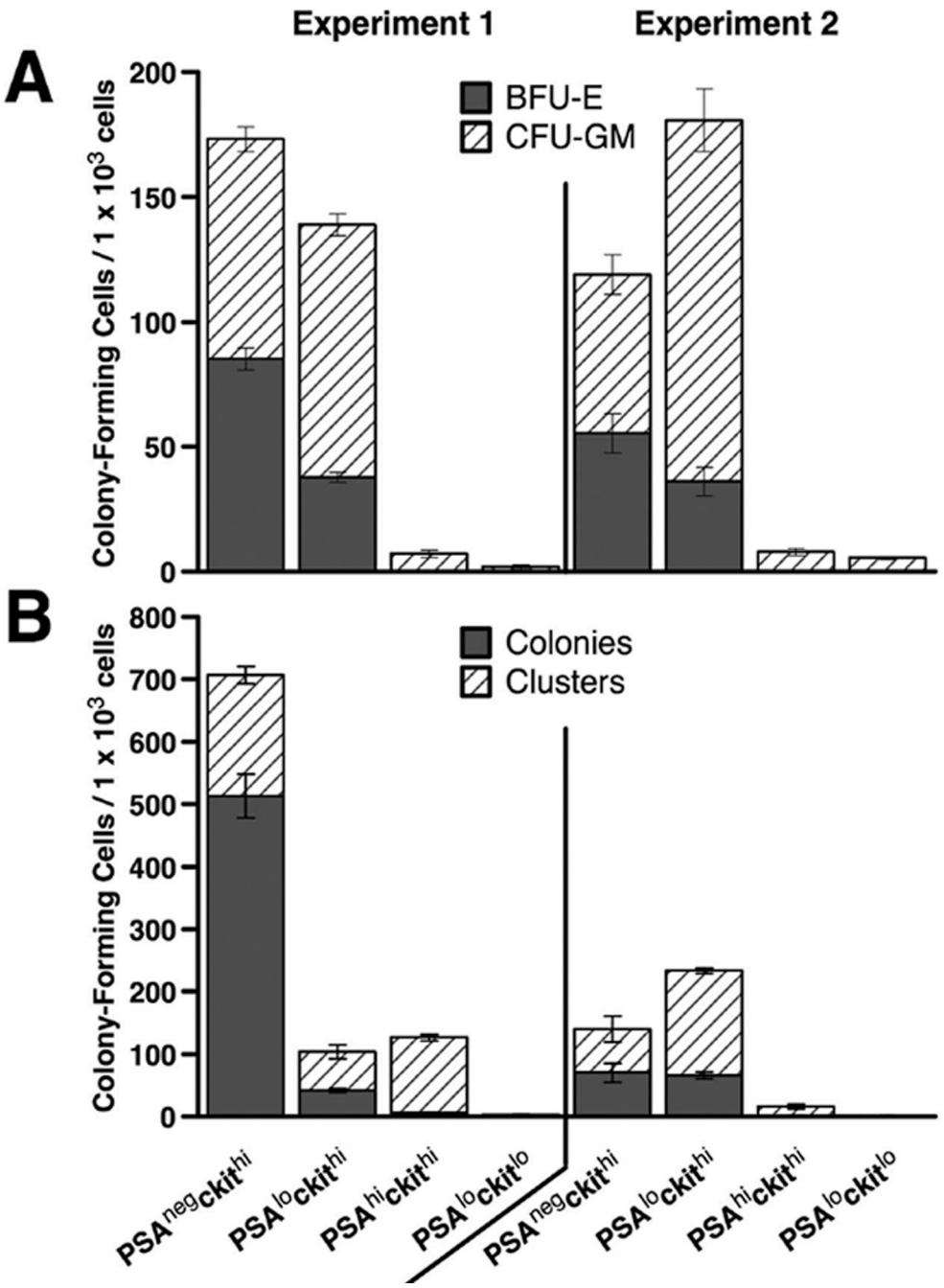

Figure 4. The PSA^{neg}/Kit^{hi} and PSA^{lo}/Kit^{hi} subsets contain erythroid and myeloid progenitors

PolySia (PSA)/cKit-defined subsets were sorted from wild-type bone marrow and plated in culture using conditions that promote erythroid (A) or myeloid (B) development. (A) Cells were maintained for 7 d in methyl-cellulose with erythropoietin, stem cell factor and IL-3, then analyzed microscopically for burst-forming units erythroid (BFU-E), and colony-forming units granulocyte-macrophage (CFU-GM). BFU-E and CFU-GM counts were combined to determine the total number of colonies formed. (B) Bone marrow cells were maintained in culture for 7 d, then scored microscopically for colonies (>50 cells) and clusters (10–49 cells). The results of two separate experiments are shown.

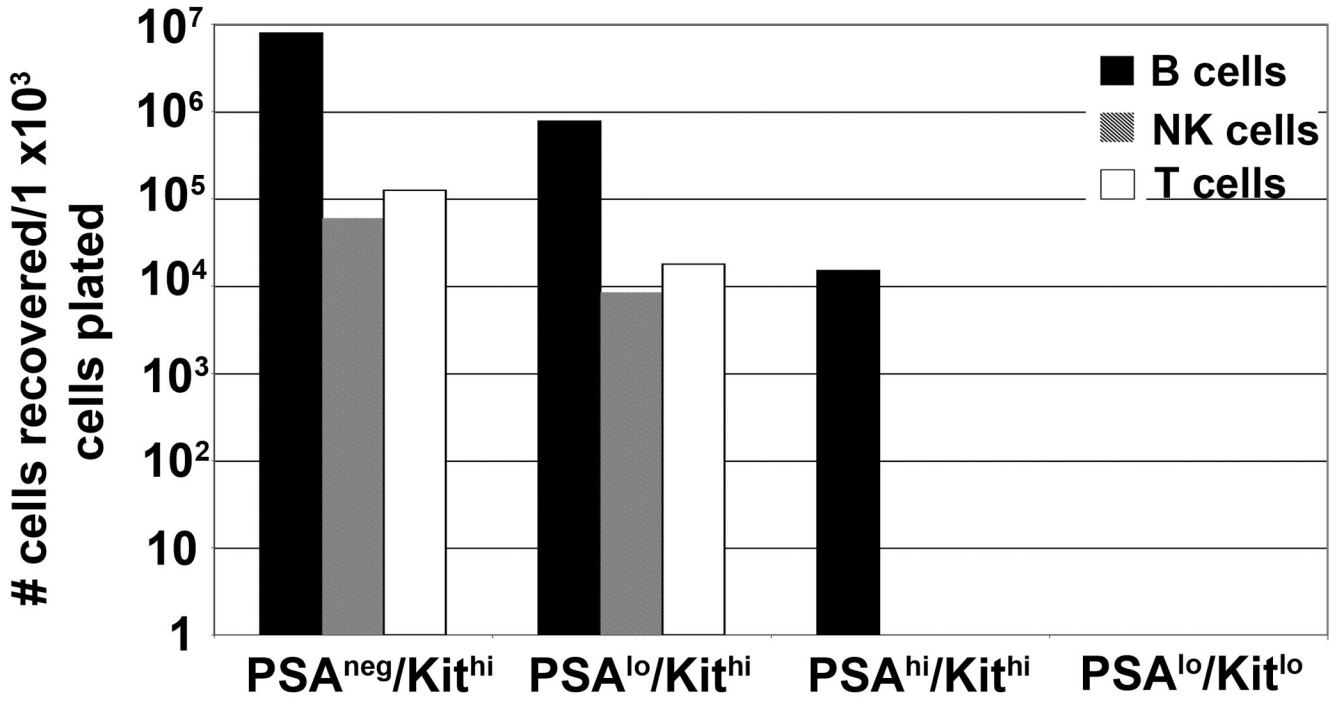

Figure 5. The PSA^{neg}/Kit^{hi} and PSA^{lo}/Kit^{hi} subsets contain lymphoid progenitors

PolySia (PSA)/cKit-defined subsets were sorted from wild-type bone marrow and placed in co-culture with OP9 stromal cells expressing either GFP and DL-1, or GFP alone. OP9-DL1 promotes the differentiation of lymphoid progenitors into T cells and NK cells, while OP9-GFP supports the development of B cells and NK cells. Differentiation was monitored by flow cytometry; results after 18 d in culture are shown. B cells were identified by B220 expression, and NK cells by cell surface DX5. T cell development was monitored by appearance of double negative stage 2 and 3 cells, identified by expression of CD44 and CD25. Representative data from one experiment are shown. The experiment was repeated three times with similar results.

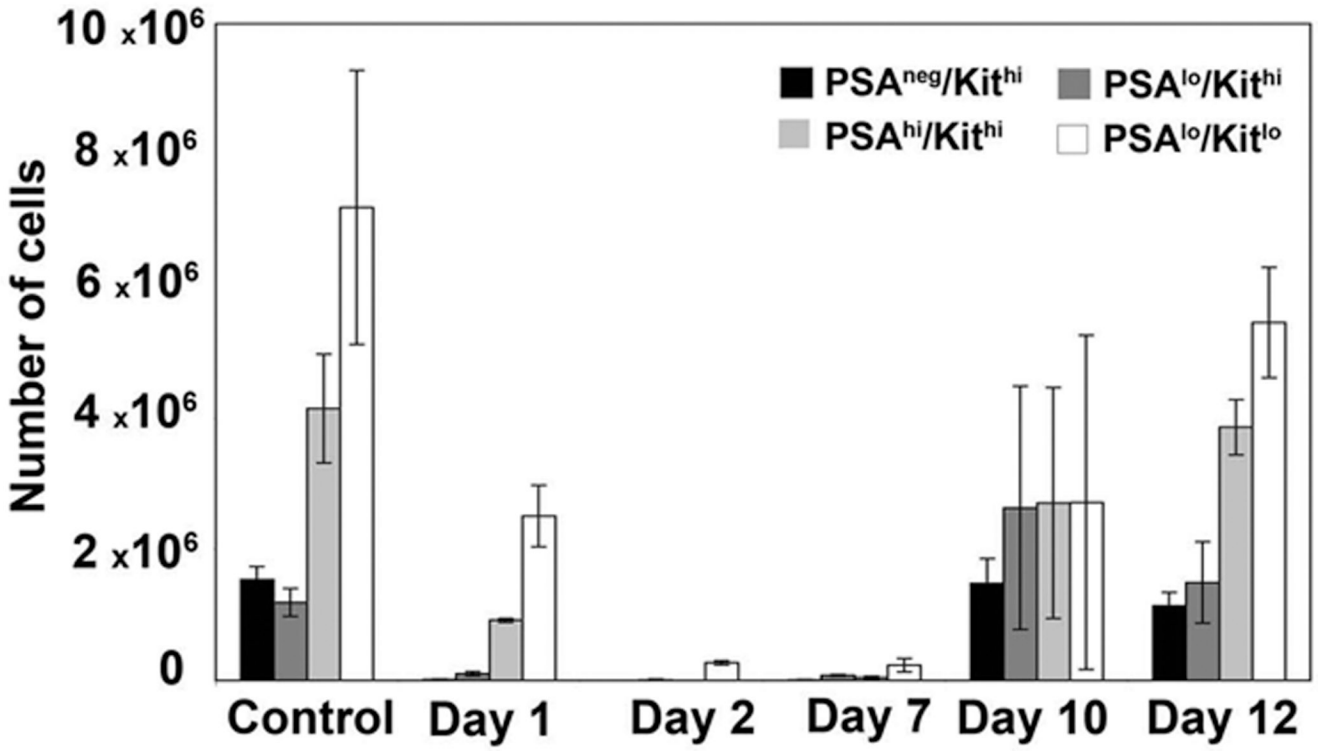

Figure 6. Development of the polySia (PSA)/cKit-defined subsets is temporally linked

Wild-type mice were injected with a single dose of 5-FU to deplete cycling cells, and then sacrificed at various intervals over a 12-day period. The loss and restoration of the PSA/cKit-defined subsets was monitored by flow cytometry.

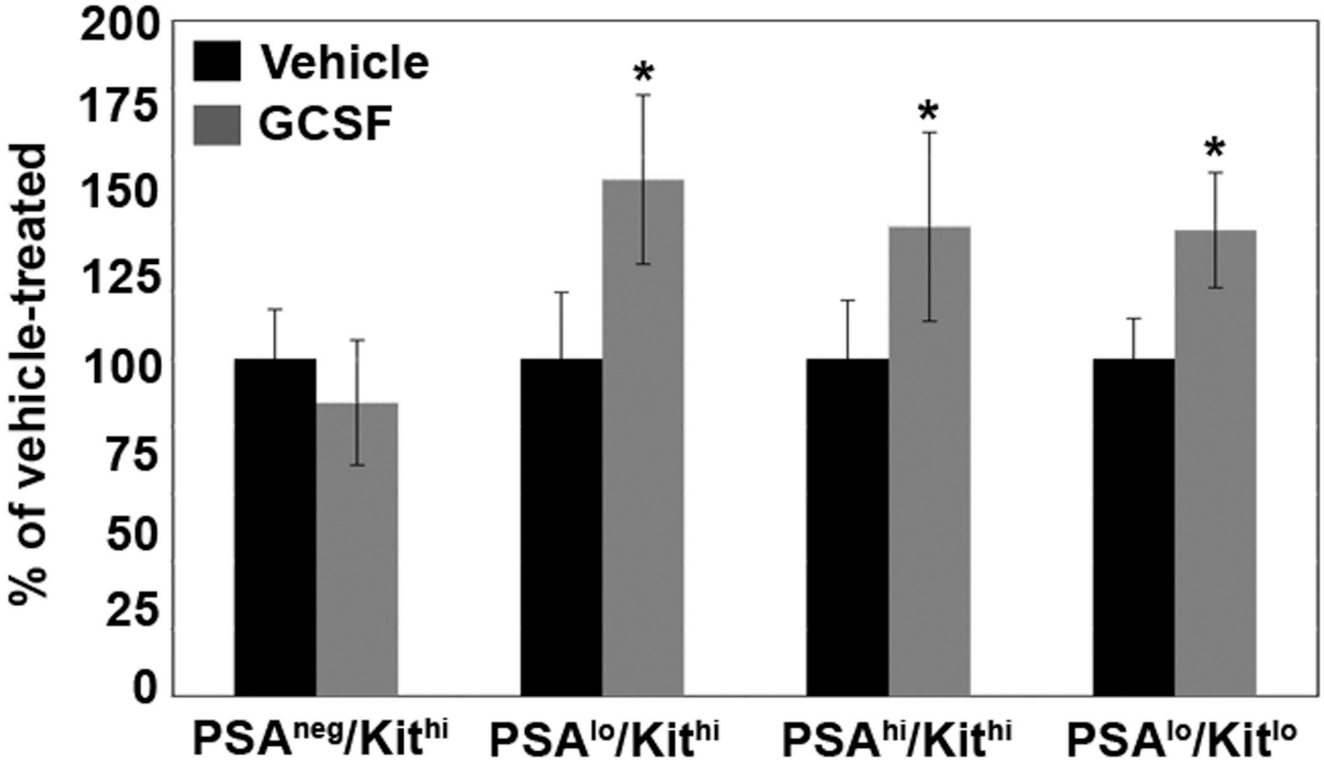

Figure 7. G-CSF increases the production of the PSA^{lo}/Kit^{hi}, PSA^{hi}/Kit^{hi} and PSA^{lo}/Kit^{lo} subsets

Wild-type mice were injected every 24 h with either vehicle alone or vehicle containing 2 μg of G-CSF. Animals were sacrificed after 5 d and polySia/cKit-defined bone marrow subsets were monitored by flow cytometry. The change in percent of total bone marrow was calculated for each population. The results of two separate experiments were combined and plotted in this graph. * $p \leq 0.007$

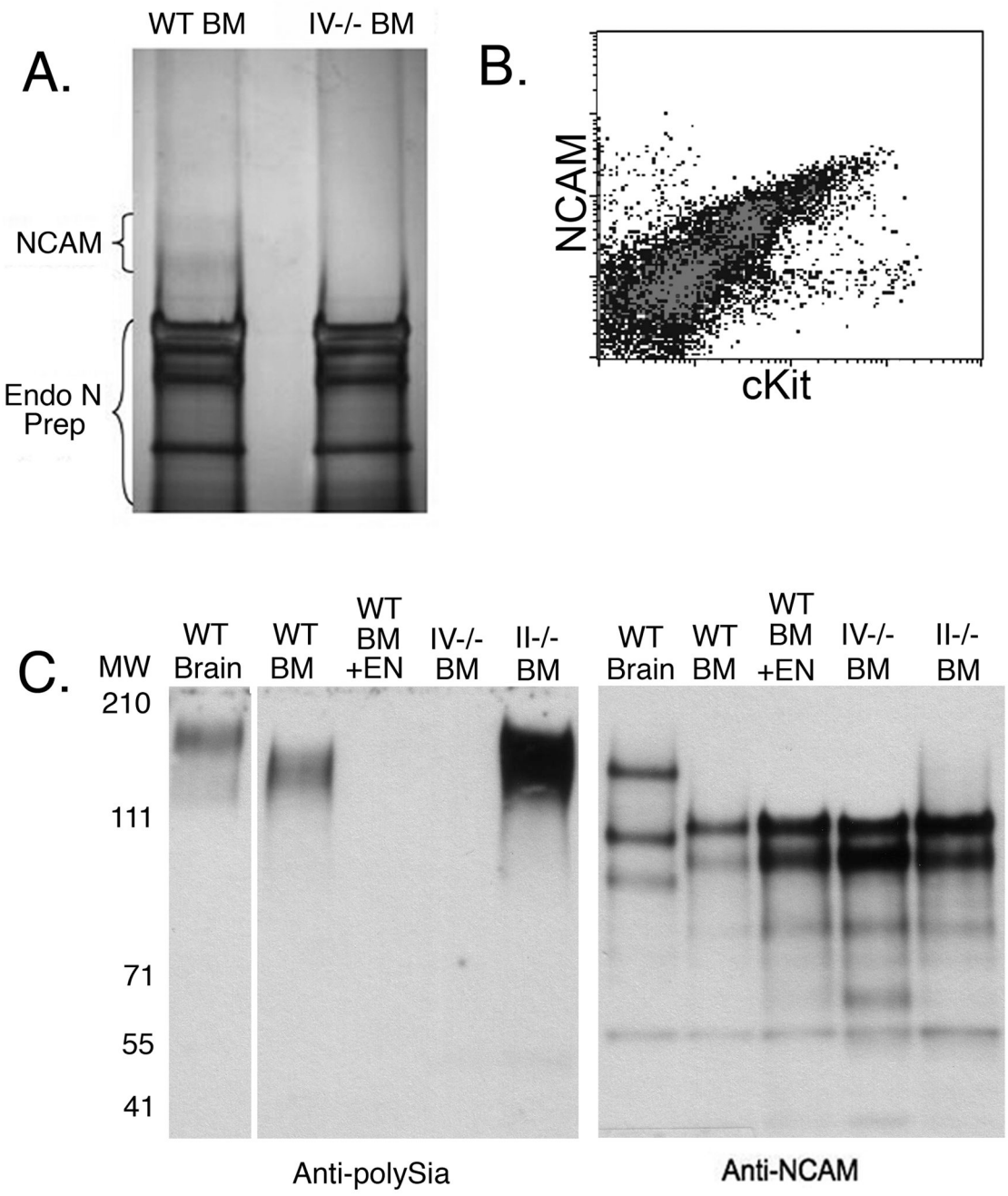

Figure 8. NCAM on the surface of mouse bone marrow cells is the scaffold for polySia

Polysialylated proteins were immunoprecipitated from lysates of wild-type (WT) or ST8Sia IV−/− (IV−/−) bone marrow (BM) cells and Endo-N-treated (A). Recovered proteins were silver stained and two bands were visible in wild-type, but not ST8Sia IV−/− samples. The bands were isolated and both were identified as NCAM, on the basis of two peptides each, by mass spectrometry. Flow cytometry using anti-NCAM and anti-cKit on wild-type mouse bone marrow cells showed NCAM was expressed on populations that were analogous to those observed by staining with anti-polySia and anti-cKit (B). Immunoblotting with anti-polySia and anti-NCAM mAbs showed a polySia signal in WT and ST8Sia II−/− BM, but not ST8Sia IV−/− BM. In contrast, an NCAM signal was observed in association with all the samples (C).

Adult WT brain lysate was used as a positive control for both polySia and NCAM signals, and Endo-N-treated (+EN) wild-type bone marrow was used as a negative control for polySia expression. Three major isoforms of NCAM were visible in brain lysates, while two (of ~140 and ~120 kDa) were present in bone marrow samples. Note that the polysialyated bands migrated with a lower mobility than those recognized by anti-NCAM, as only a fraction of this molecule carried these specialized glycans.

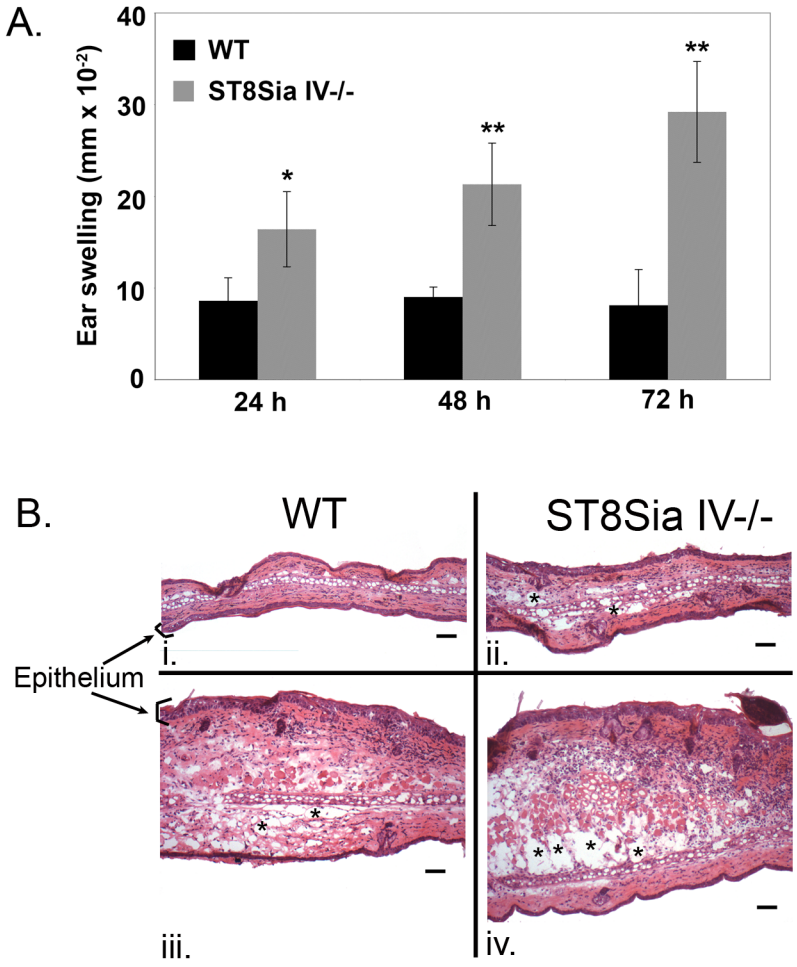

Figure 9. The contact hypersensitivity response is excessive in ST8Sia IV−/− mice

Wild-type and ST8Sia IV−/− mice were sensitized to DNFB. One week later the left ear was treated with DNFB and the right ear with vehicle alone as a negative control. We assessed the inflammatory response by measuring ear thickness with digital calipers at 24, 48 and 72 h (A). Each ear measurement was taken three times. The data represent the average ear thickness ± SD for the DNFB-treated ears of all mice (n = 3 WT, n = 3 ST8Sia IV−/−). At each timepoint, ST8Sia IV−/− mice had significantly more ear swelling than did wild-type animals (* $p = 0.01$; ** $p \leq 0.001$). Histological analyses showed excessive tissue damage observed in ST8Sia IV −/− mice as compared to wild-type mice (B). Vehicle- (B i and ii) and DNFB-treated (B iii and iv) ears were removed, fixed, sectioned and stained with hematoxylin and eosin for histological analysis. Asterisks denote areas of edema, which appeared as empty spaces. Bar = 60 um.

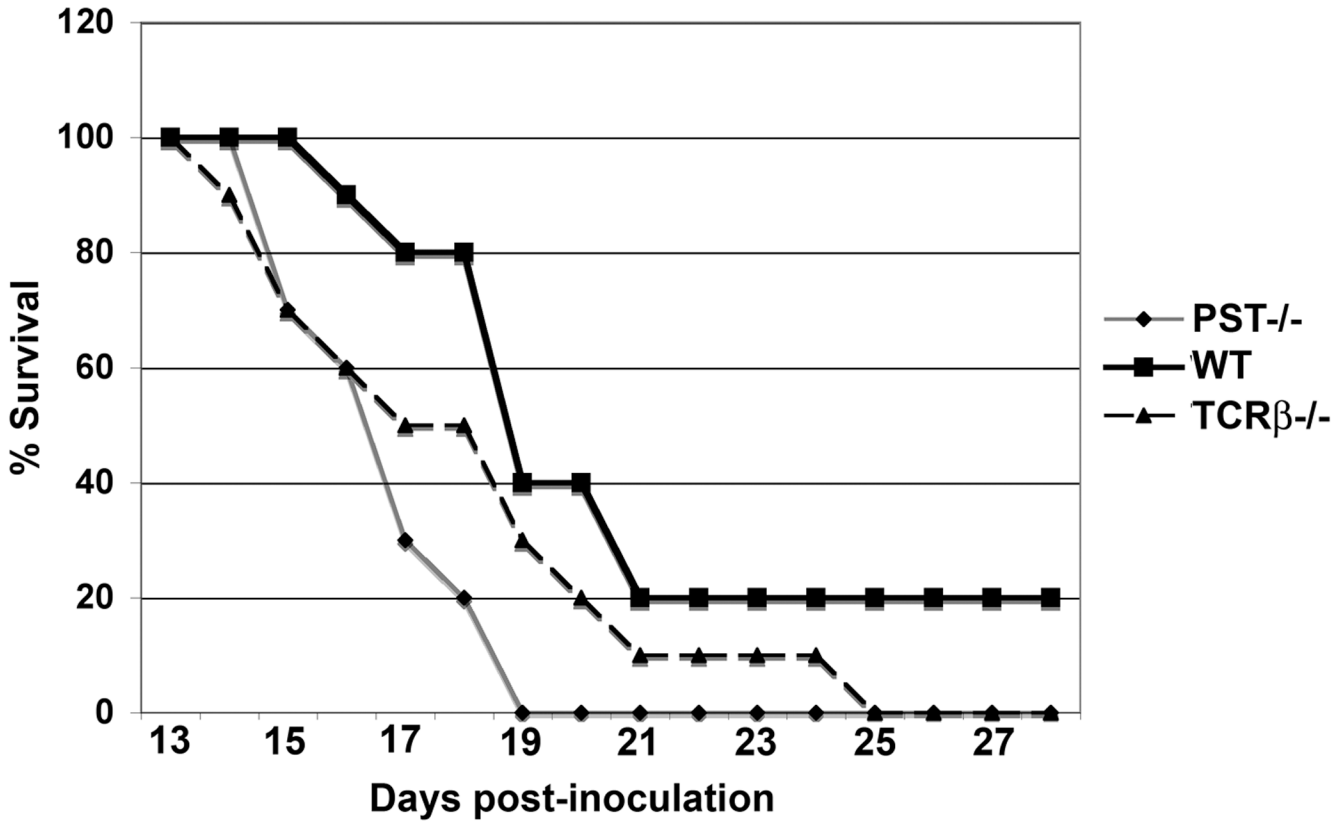

Figure 10. RMA tumors grow faster in ST8Sia IV−/− mice than in wild-type animals

Wild-type, ST8Sia IV−/−, and TCRβ−/− mice (negative controls for immunocompetence) were injected subcutaneously with 10^4–10^5 RMA cells. When tumors became ulcerated, or grew larger than 1.5 cm, or mice lost >20% of their original body weight, animals were sacrificed. Animals surviving more than 60 d were considered tumor-free; all deaths are plotted on the graph. There was a statistically significant difference in survival rates between wild-type and ST8Sia IV−/− animals ($p = 0.02$, two-tailed Mann-Whitney test).

Table I

	% Lin−	% CD34+	% CD11b+	% Gr-1 lo	% Gr-1 hi
PSA^{neg}/Kit^{hi}	55 ± 11	65 ± 6	9 ± 0.3	9.8 ± 0.9	2 ± 1.7
PSA^{lo}/Kit^{hi}	7.4 ± 1.7	95 ± 2	61 ± 0.55	31.4 ± 0.9	27 ± 1.6
PSA^{hi}/Kit^{hi}	0.02 ± 0.17	66 ± 2	96 ± 0.2	73 ± 5.2	9 ± 0.01
PSA^{lo}/Kit^{lo}	0.26 ± 0.25	21 ± 3	99 ± 0.3	38.6 ± 0.1	59 ± 0.1

n=3

The expression of the following antigens was also analyzed (data not shown): CD150, CD48, CD244.2, HSA, FLT3, IL-7R, Thy1, CD27, TER119, B220, CD3, CD4, CD8, TCRβ, TCRγδ, NK1.1, CD11b, CD11c, CD25, and CD36.

Table II

	Bone marrow		Spleen			
	TER119	**Gr-1**	**Gr-1**	**CD14**	**DX5**	**B220**
PSA^{neg}/Kit^{hi}	59 ± 47	117 ± 88	320 ± 58	172 ± 108	29 ± 18	249 ± 194
PSA^{lo}/Kit^{hi}	33 ± 5.6	50 ± 34	273 ± 47	162 ± 45	26 ± 11	206 ± 47
PSA^{hi}/Kit^{hi}	1.2 ± 0.8	2.1 ± 0.3	10.7 ± 10.7	6.6 ± 7.7	1.4 ± 1.8	9 ± 15
PSA^{lo}/Kit^{lo}	1.6 ± 0.6	2.1 ± 0.7	0.5 ± 0.9	0.08 ± 0.13	0	1.9 ± 1.1

Number ($\times 10^3$) of recovered GFP+ cells expressing the designated cell-surface antigen/thousand transferred cells.